

**SLOT MILLING OF AA7075 REINFORCED WITH NANO SILICON
CARBIDE PARTICLES – AN EXPERIMENTAL AND FINITE ELEMENT
APPROACH**

Prakash Chakrapani^{1*}, Prakash Jayaraman²

¹ Department of Automobile Engineering, School of Engineering and Technology, Surya Group of Institutions, Anna University, Vikiravandi – 605652, Villupuram District, Tamilnadu, India.

² Department of Mechanical Engineering, School of Engineering and Technology, Surya Group of Institutions, Anna University, Vikiravandi – 605652, Villupuram District, Tamilnadu, India.

Received 26.08.2024.

Revised 19.3.2025.

Accepted 24.3.2025.

<https://doi.org/10.2298/CICEQ240826006C>

*Corresponding author email: prakashc@suryagroup.edu.in, Mobile number: +919444108957

Abstract

In the current trend, industries prefer to optimise machining processes using finite element-based machining simulation techniques. Aluminium alloy 7075 (AA7075) strengthened with nano Silicon Carbide particles (nSiCp) is utilized by industries as they exhibit good physical and mechanical properties. Slot milling is the essential machining operation to convert the component to the designed shape and size. However, excellent knowledge is required in selecting the appropriate machining parameters such as cutting velocity, feed and cutting tool material to ensure the quality of the components milled. In this research work, slot milling operation is carried out in the sample plates of AA7075 fortified with nSiCp content to 1.5% of the weight. A 3D Finite Element Model (3D FEM) is developed using ABAQUS software for simulating slot milling operations to understand the influence of machining parameters on cutting forces, chip formation and chip morphology. The cutting force signals predicted by 3D FEM correlates 85 to 90 % with experimental data. The maximum shear stress of 175 MPa and Von Mises stress of 459 MPa were observed at the tool-workpiece interface. This validated 3D FEM facilitate to visualize and investigate the milling process and assists in selecting appropriate machining parameter settings. The effects of cutting velocity and feed on cutting forces, chip characteristics, stress and chip formation are reported.

Keywords: Aluminium nanocomposite; Slot Milling; 3D FEM; Cutting forces; Chip morphology

Highlights of the research:

The Aluminium nanocomposite is fabricated, and machinability studies are performed.

The nSiCp reinforcement improves the mechanical characteristics of the AA7075 material.

Experimental slot milling is performed and cutting force, chip morphology studies are carried out.

Slot milling is simulated using 3D FEM and the Experimental Vs. 3DFEM correlation studies are done.

The influence of cutting parameters on the machinability of the nanocomposite is evaluated.

Introduction

The machinability of the aluminium nanocomposite investigated in this research work is an aluminium-based Metal Matrix Composite (MMC) reinforced with nano SiC particles (<100 nm) to improve the mechanical properties of AA7075 based on the requirements in modern industries. These MMCs are extensively utilised by the automobile and aircraft industries due to their intrinsic mechanical properties when compared to steel such as being lighter in weight, ductility, good stiffness, fracture toughness and corrosion resistance even at extreme operating conditions. This attracts the attention of researchers and makes it necessary to investigate the machinability of aluminium-based nanocomposites [1-3]. It has been projected that, by the year 2025 the increase in utilization of aluminium in a car will reach 250 kg from 150 kg as of now [4].

The aluminium-based MMCs reinforced with SiC particles have potential applications in the aviation and transport fields, bearings, fins of aircraft fuselage, struts of avionics systems and aero engine compressor blades [5], brake wheels of four-wheelers and high-speed trains [6]. The milling process is mostly utilised to bring the raw material / semi-finished product to the designed shape and size. However, machining defect-free products/components with good quality is challenging in aluminium nanocomposite due to the nSiCp reinforcement in aluminium nanocomposite, which is greatly influenced by the machining parameters selected and the machining conditions [7]. The challenging issues in the milling of aluminium-based MMCs are dimensional inaccuracy, chip built-up edge, unstable cutting forces due to reinforcement material (nSiCp), higher cutting forces, surface roughness, stress concentration, accelerated tool wear, exit burr formation, surface finish and reduction of fatigue life etc. Hence, ensuring the dimensional accuracy, quality and reliability of the machined components by eradicating these damages caused while machining is very much essential. Moreover, it is also mandatory to explore the basics of machining the MMCs by investigating the importance of the volume and distribution of the nano SiC particles on the damage mechanism of MMC, the interaction of the mill tool with SiC particles and the effect of machining parameter combinations (feed rate, depth of cut, cutting velocity, etc.) on dimensional accuracy, quality of the machined surface and ease in machinability. This motivates the engineers, researchers and industries to investigate on milling of aluminium-based MMC to understand the effects of SiC reinforcement in its machinability [8].

To eradicate the machining difficulties experimental studies are mandatory which is time-consuming and highly expensive, particularly at extensive machinability metrics (i.e. combination of machinery, tool material, tool geometry, machining parameters and machining environment selected for machining studies) [9]. However, interpreting the experimental results highly depends on the quality of the machinery and data acquisition equipment used. Moreover, it is essential to have a

complete understanding of the behaviour of metal matrix composites while machining under different machining parameter combinations, which could optimistically ease the machining operations. Hence, the researchers and industries wish to utilise 3D FEM for investigating the machining of MMCs. Using 3D FEM the complex milling process is simulated in three dimensions to predict the cutting forces and cutting stress and to visualize for understanding the chip formation process.

Bhuvanesh et al. [10] reported the influence of machining parameters on surface roughness while performing slot milling in aluminium-based hybrid composite strengthened with SiC and B₄C materials. The reduction in plastic deformation is observed with the increased percentage of reinforcement particles while machining. Hence, it is suggested to perform slot milling operations at larger cutting velocities and minimum feed rates to remove the reinforcement material easily and to achieve a good surface finish. Ma et al. [11] performed the experimental milling in Aluminium alloy 7075 and reported the cutting forces, stress and chip morphology. The Finite Element Analysis (FEA) simulation studies are also made and the results were correlated with the experimental findings and seem to be similar. Davoudinejad et al. [12] simulated the slot milling process using a 3D FE model for different machining parameter combinations and reported the cutting forces, chip morphology, cutting temperature and stress obtained from experimental and Finite Element (FE) studies.

Raghuvaran et al. [13] reviewed the mechanical properties of aluminium-based MMC. It is reported that AMCs find extensive applications in the aerospace and automobile industries and thereby they replace conventional metals and materials. Reinforcement of SiC 10 % of weight with AA7075 increases the tensile strength of the composite by 9.67% which creates interest among researchers. Cui et al. [14] established a 3D FEM using ABAQUS/Explicit and simulated the milling operation in aluminium alloy 7075-T7451. The authors also reported the cutting force data and chip morphology. Umer et al. [15] investigated the subsurface damages caused while machining the aluminium-based MMCs using a 2D FE model. The researchers revealed the machined surface damages such as damage depth, particle debonding and the effects of cutting velocity and feed on the quality of the machined surface. The researchers also developed 2D micromechanical and 3D equivalent homogeneous models to simulate the orthogonal cutting of aluminium- based (Al359) SiC reinforced MMC. The EHM model proves its ability in predicting and simulating the cutting process effectively by Umer et al. [16]. Zhou et al. [17] developed a 2D FEM and simulated the orthogonal cutting process. The researchers reported the effects of machining parameters on residual stress, surface roughness, dimensional accuracy and shape.

Prakash et. al. [18] developed a 3D FEM to simulate the slot milling process in unidirectional Carbon fiber reinforced polymer composites. The investigation reveals how the machining parameters such as cutting velocity and feed influence cutting forces, stress, chip formation, chip morphology and machining-induced damages. The developed 3D FEM also assists in selecting

appropriate machining parameter settings to enhance the machining quality and dimensional accuracy. Prakash et al. [19] utilised the developed 3D FEM from the earlier research work and simulated the high-speed milling of AA7075 Reinforced with nB₄Cp. The 3D FEM-based milling simulations suggested milling the MMC with higher cutting velocity and at a lower feed rate. Pedroso et al. [20] concisely summarised the utilisation of FEA strategies for predicting the machining process in INCONEL material and briefed the recent advancements in machining simulations from 2013 to 2023. The review work carried out by the authors revealed the necessity to investigate more for developing new 3D FEMs for enhancing their accuracy and reliability.

Dodla et al. [21] studied conventional and ultrasonic vibration-assisted machining of aluminium alloys, titanium alloys and Inconel – 718 materials. Numerical methods of both the machining techniques reported the cutting forces, thermal effects and chip morphology. The authors suggested to utilising UVA machining to reduce machining forces and machining-induced damages. Deshmukh et al. [22] reported a brief review on the machining of aluminium-based Metal Matrix Composites which guides the researchers to work on cutting tool methodology. The authors reported the recent advancements in the machining of MMCs in their review article. The authors also highlighted the various types of MMCs available and their inherent mechanical behaviours which suit specific industry applications and also create the interest for the researchers to evolve new hybrid MMCs. Liangchi et al. [23] reviewed the recent advancements in modelling the machining of fiber reinforced and particulate reinforced composites. The review reveals that the accuracy and reliability of the numerical model highly relies on the correctness of constitutive models incorporated in the FEM.

Prakash et al. [24-30] have presented a recent work focusing on developing 3D FEM and simulated the drilling and slot milling operation in GFRP, CFRP composites, Aluminium-based MMCs and investigated the influence of cutting velocity and feed on cutting forces, stress, chip formation, and chip morphology. These researches provided an insight to understand and visualize the drilling and slot milling process in those composites. The experimental findings and 3D FE predictions are excellent in similarity and the developed 3D FE model is novel and reliable in simulating and predicting the optimum machining parameter settings. Prakash et al. [31, 32] the co-author of this fabricated and investigated the mechanical properties of aluminium nanocomposite and also studied the quality of the holes drilled in the fabricated composite. The researcher suggested AA7075 with 1.5% nSiCp composition is an optimum MMC for wider applications. Since, it shows improved mechanical properties as expected by the aerospace industries [33, 34].

The literature review reveals that most of the researchers concentrate on developing some 2D and 3D FE Models and simulated the milling process. From the earlier research, it is understood that 3D FE Models are comparatively more reliable and effective in predicting the cutting force data, chip formation process, chip characteristics and machining-induced damages than 2D FE models.

However, the 3D FEM developed so far is not so reliable and efficient in simulating the milling operation in MMCs. Since, it requires huge computation resources, more knowledge in Finite Element studies in developing 3D FEM, time and complexity in the geometry of the modern tools. Moreover, there are no correlation studies on chip failure and chip characterization from an experiment Vs. FEM simulation particularly in 3D.

Therefore in this research work, slot milling experiments were done in aluminium nanocomposite, followed by the development of a 3D FEM in Abaqus/Explicit. The experimental and FEM simulation results were correlated for FEM validation. Moreover, this validated 3D FE Model is an effective and reliable virtual tool to assist in selecting the optimum machining parameter settings [35] to ease the slot milling process thereby ensuring the dimensional accuracy and quality of the components milled by minimising the machining-induced damages such as crack formation and surface finish.

METHODOLOGY

Material Selection

In this research work, the Aluminium nanocomposite (AA 7075 + 1.5% nSiCp) is fabricated by introducing the nano-sized SiC particles as reinforcement into the matrix of AA7075 aluminium alloy. The reinforced particles (nSiCp) used in this research work are in the 45 - 65 nm range. AA7075 is the matrix material which owns excellent mechanical properties such as less density, good thermal behaviour, high tensile strength, and better surface. The nano Silicon Carbide particles possess good mechanical behaviour such as heat conductivity, good wear resistance, low thermal expansion coefficient and good temperature resistance. Hence, SiC is used as the reinforcement material to enhance the mechanical properties of AA7075. The composition of the AA 7075 + 1.5% nSiCp can be referred from the articles of the co-author [31, 32].

The Aluminium nanocomposite is made up of a stir casting method (shown in Figure 1 a.) with five different AA7075 + nSiCp compositions and mechanical characterization studies were carried out by Prakash J et al. [32]. The mechanical properties of the aluminium nanocomposite with the composition, of 985 grams of AA7075 + 15 grams of nSiCp (1.5% by weight) are comparatively outstanding. Therefore, based on the literature review [29, 30] and the former research work carried out by the co-author, the suggested composition (AA 7075 + 1.5% nSiCp) is preferred for the current research work. The Field Emission Scanning Electron Microscope (FESEM) image of the fabricated aluminium nanocomposite is taken using CARL ZEISS (Model: sigma with gemini column) FESEM equipment. This equipment with features such as a resolution of 1.5 nm, In lens Detector, SE₂ detector

and BSD detectors is good enough to capture the surface topography of the fabricated MMC at the required resolution.

The captured FESEM image shown in Figure 1 b reveals how SiC nanoparticles are distributed within AA7075 matrix material by Prakash J et al. [32]. The fabricated aluminium nanocomposite is a very good alternative to steel. The former research carried out by the co-author reveals the enhancement in the mechanical properties, when AA7075 is reinforced with 1.5 % nSiCp. The mechanical properties of AA7075 with 1.5 % nSiCp are found to be excellent from the earlier studies [32].

Figure 1

Experimental Setup

The slot milling experiments were carried out in BMV 51 TC24 vertical milling centre with the machining parameters listed in Table 1. Figure 1 c shows the experimental setup which comprises of milling centre, tool, workpiece and the mill tool dynamometer with a data-acquisition system. The TiAlN coated solid carbide end mill cutter is used for experiment studies which was supplied by Ultimate Machine Tools, Chennai, India. End mill tool – CoroMill model which was specially designed for milling composites is used for this investigation [26]. Moreover, an end mill cutter with a helix angle of 30° and a point angle of 130° to 140° is selected for this experimental investigation as it is highly preferred by recent researchers and tool manufacturers [9, 25, 38].

The slot milling experiments were conducted with different cutting velocities and feed combinations presented in Table 1. However, the machining parameter values are selected based on the suggestions by the researchers and the information from the earlier investigations carried out by the authors. The key objective of this research is to perform chip morphological studies to evaluate, report the chip formation and machinability of aluminium nanocomposite and to correlate with the 3D FEM simulation studies. This chip correlation study ensures the reliability of the developed 3D FEM. Hence, selecting the moderate and below moderate cutting velocity and feed rate combinations is mandatory for this current research work (given in Table 1). Since, the chips obtained for these machining parameter combinations are good enough to visualise and categorize for correlating with FEM results [19, 38]. However, the higher cutting velocity with a lower feed rate is preferred to minimize the cutting forces [9] whereas this cutting parameter combination produces very fragile and tiny chips which resemble dust particles. Moreover, these chips are found to be not suitable for performing morphological studies. Cutting forces are recorded using a SYSCON mill tool dynamometer which is supplied by SYSCON Instruments Private Limited, Bangalore, India (shown in Figure 1 c). The strain gauge based milling dynamometer (Max Load capacity – 500 Kgf, Model

Name – SPL, Type - strain gauge) with full bridge component for each direction was utilised for this experimentation. The acquired analog signal is converted and communicated to the computer through an analog – digital converter, which is then displayed in the form of graphical output to capture the cutting force data while performing experimental slot milling.

Table 1

Finite Element Analysis

FEA Methodology

In this research work a Lagrangian 3D FEM was developed to simulate and visualise the slot milling operation in Aluminium nanocomposite using the ABAQUS FEA software [39]. 3D FE simulation trials are performed for different machining parameter combinations given in Table 2 and the critical cutting force, stress and chip formation phenomenon were predicted (Described in the results and discussion section). The milling simulation created by the 3D FEM technique helps in visualising the interaction of the end mill and the MMC very effectively and it provides an insight into the machinability of the aluminium nanocomposite from a different perspective. Moreover, 3D FEM is the only effective technique to visualise the dynamic metal cutting process which involves the interaction of complex tool surfaces with workpiece [8].

3D model of tool and aluminium nanocomposite.

The three-dimensional model of the end mill tool with two flutes is modelled in CATIA V5 using the part module [40] (shown in Figure 2 a.) as per the tool nomenclature described in the research article [26]. The 3D model of the four fluted end mill cutter was modelled in CATIA V5 and saved as interactive Graphics Exchange System (IGES) format which is imported to ABAQUS to develop 3D FEM. The 3D equivalent homogeneous model ($25 \times 25 \times 10$) mm³ of the aluminium nanocomposite is created as shown in Figure 2 b using the part module in ABAQUS.

Figure 2

3D Finite Element Model

The 3D FEM was developed by assembling and positioning the 3D model of the end mill cutter and the MMC. Furthermore, tool and MMC models were discretized with suitable element types and element numbers based on the requirement to simulate the machining process optimistically (the FE input details are given in Table. 2). Element mesh optimisation (selection of suitable mesh size) of the 3D FEM is mandatory to simulate the machining process effectively to compromise between the available computational resources, solving time and the efficiency & reliability of the FE results. The

3D model of the end mill tool is considered a rigid body [8, 19, 39] to reduce the computing efforts. Moreover, the mechanical properties of the mill tool are superior to the MMC and in addition tool wear studies are not in focus in the current research work which is to be considered in our future investigations.

Table 2

The assumptions in developing the 3D FEM for performing slot milling simulation studies are,

- The composite model developed for this current study is an Equivalent Homogeneous Model (EHM).
- The 3D model of the twist drill is assumed to be a rigid body since tool wear is not considered in the current investigation in order to reduce the computational efforts.
- Tool wear is not considered in this investigation, which is not the main focus of the study.
- In friction modelling the frictional stress developed in the tool-workpiece interaction zone during slot milling operation is proportional to the normal stress.
- Thermal issues are not considered as the temperature recorded during slot milling experimentation is less than 75⁰C only, which is kept as our future scope of study.

Material modelling and failure criteria of AA 7075 + 1.5% SiC

The fabricated MMC with the chemical composition listed in Table 3 shows excellent mechanical properties. Johnson's cook failure model available in the material model of the ABAQUS software was incorporated in the developed 3D FEM to simulate the plastic behaviour of the aluminium nanocomposite. The Johnson - cook failure criteria (Equation 1) is preferred for this investigation because it is good enough to predict the cutting forces, stress, chip morphology, flow stress and plastic deformation for ductile materials and metals and it is widely used by researchers for machining simulation studies [26,41,42]. The features of the J-C parameters are as follows,

Advantages of J-C failure model in 3D FEM-based machining simulation [39]

- J-C failure model is best suited for materials which experience high strain rate, large strain and larger deformation.
- It also considers plasticity, flow stress, work/strain hardening and temperature softening of metallic materials.
- The J-C failure model is excellent for exhibiting the material behaviour under dynamic (dynamic explicit) situations like machining simulation.

- Supports progressive degradation of material stiffness and removal of mesh elements by incorporating appropriate damage initiation and evolution factors. This assists in chip formation and separation in 3D FEM machining simulation.

Disadvantages and Limitations of J-C failure model in 3D FEM-based machining simulation [39]

- The seven parameters need to be determined for each structural material, which makes the investigation costlier and time-consuming.
- The solving time of the machining simulation using 3D FEM takes a long time.
- It is mandatory to correlate the simulation results with experimental results to be validated.

The Johnson - cook failure criteria is utilised to define the mechanical properties (listed in Table 3) of the aluminium nanocomposite (given in Table 3), J-C constitutive material parameters (listed in Table 3) and J-C damage parameters d_1 to d_5 in Table 3 [42-44]. The damage evolution and element removal are initiated by Johnson-cook damage initiation criteria and at the damage initiation parameter, $d = 0.001$ which facilitates the FEM to activate chip formation [35]. Enough preliminary trial simulation studies were carried out and appropriate damage initiation parameters were selected.

$$\sigma = (A + B\varepsilon^n) \left(1 + C \ln \frac{\varepsilon_1}{\varepsilon_0} \right) \left[1 - \left(\frac{T - T_r}{T_m - T_r} \right)^m \right] \quad (1)$$

In which, the constants A, B, C, n, m and T are listed in Table 3.

Table 3

Boundary conditions

The loading conditions (cutting velocity and feed rate combination listed in Table 1) and the boundary conditions that prevailed in the real-time slot milling process were applied to the 3D FEM [24, 25]. The aluminium nanocomposite–workpiece FE model is constrained for all degrees of freedom for the outer four sides and the bottom surface (as shown in Figure 2 b.) The tool is constrained for degrees of freedom except feed direction (X axis) and tool rotation axis (rotation along Z axis). Furthermore, the feed rate and spindle speed values were given as input to the reference point which is created at the tip of the end mill cutter as shown in Figure 2 b.

Interaction properties

The coulomb friction concept (sliding and sticking friction) is introduced in the developed 3D FEM which characterises the interaction between the tool and the aluminium nanocomposite (governed by equation 2). This interaction behaviour characterises the frictional effect produced while performing

slot milling operations in the MMCs [45]. The friction coefficient between the composite and end mill cutter is taken as 0.6 [8, 42].

$$\tau_n = \mu\sigma_n \quad (2)$$

RESULTS AND DISCUSSION

Cutting force

The elevated cutting forces developed while machining the MMCs cause machining-induced damages such as surface roughness, dimensional inaccuracy, residual stress, internal cracks etc. Moreover, the cutting force is the key parameter which influences more in chip formation, stress, chip morphology and tool wear while performing slot milling operations in the aluminium nanocomposite. The machining accuracy, quality and reliability of the machined components are to be ensured by minimising the milling-induced damages by reducing these cutting forces. However, minimising the cutting forces while milling is quite challenging, which creates interest for the researchers to investigate machinability studies of MMC. However, evaluating the exact magnitude of critical cutting forces is very difficult which depends on the experimental procedures and quality of the testing equipment utilised [8]. On the other hand 3D FEM technique is the only efficient method to predict these critical cutting forces by simulating the slot milling operation.

Figure 3 a, b reveals a fluctuating pattern in the cutting force profile since the cutting edge angle varies with respect to the reinforced nano SiC particles while milling the aluminium nanocomposite. Whenever the cutting edge of the end mill interacts with reinforcement material (nano SiC particle) the magnitude of the cutting force increases since the nSiC particles are harder to break down while machining when compared to AA7075 [46]. Moreover, the AA7075 undergoes ductile failure whereas the SiC particle undergoes brittle failure [17]. The cutting force profile acquired from experimental and 3D FE simulations at $V_c = 47.1$ m/min and $f = 150$ mm/min is displayed in Figure 3 b.

Figure 3 c, d shows the critical cutting forces generated for the corresponding cutting velocity and rate of feed (also listed in Table 4). Table 4 displays the cutting force components F_x , F_y and F_z for different cutting parameter combinations. It is also observed that the infeed force, F_x and the cross-feed force, F_y is comparatively higher than the thrust force, F_z . When the slot milling operation is carried out at a higher cutting velocity the cutting forces developed are minimal and vice-versa. Hence, it is highly recommended to perform the slot milling operation in aluminium nanocomposite at higher cutting velocity or lower feed/tooth to minimize the machining-induced damages caused due to critical cutting force [9]. The critical cutting force values captured from the experimental investigation and 3D FE simulation are correlated and the similarity error is found to be in the

acceptable range [47]. Figure 3 shows the acceptable deviation of 10 to 15 % in the correlation of 3D FE and experimental results which is mainly due to the tool run-out during cutting action [12].

Figure 3

Table 4

Stress

The shearing action of the end mill cutter when it interfaces with the MMC during the slot milling operation results in chip formation and material removal [25]. Hence, investigating the shear stress developed at the tool–workpiece interface region is vital, since it is the major influencer for chip formation, chip progression and chip characteristics during the slot milling operation in the aluminium nanocomposite. The significance of the investigation on shear stress generation in the cutting zone is revealed in Figure 4 (a). The maximum shear stress (S_{12}) observed in the cutting zone is 175 MPa which effectively assists in the shearing of MMC.

3D FE simulation plots revealed that the von Mises stress obtained is 459 MPa (shown in Figure. 4 a) which is greater than the ultimate strength of the MMC listed in Table 3. The highest stress value of 459 MPa is observed in the cutting zone which is mainly due to the strength of the reinforcement material (nSiCp). Especially in the case of AA7075 reinforced with nanoparticles, more plastic deformation of the aluminium matrix is observed which is mainly due to the very high interaction frequency of the tool with the reinforcement particle. This phenomenon is lesser if the reinforcement particle size is larger comparatively by [15]. The highest stress value is observed at the root section of the milled chip (shown in Figure. 4 a) which causes the chip to be in the yielding state for some time. This phenomenon results in the formation of curved-shaped chips, lamella structure and twisted & rolled chip morphologies. Lamella structure in milled chips is observed for a few machining parameter combinations which is particularly due to the strained bands caused by the localised very high plastic von Mises stress during material removal.

Figure 4

Chip Formation Process in FEA

The 3D FEM developed is utilised and the slot milling operation is simulated which is displayed in Figure 4 b. The quality of the machined surface is a vital factor which influences the performance of the milled component from its application point of view. Achieving a good surface finish in the milling of nSiCp reinforced MMCs is very challenging since the formation of scratches and undercut is quite common [46] which could be avoided only by paying special attention to the selection of suitable cutting velocity and feed. The 3D FEM is an excellent technique in revealing the metal cutting phenomenon to visualise if any machining-induced defect occurs.

Figure 4 b reveals the ability of 3D FEM in simulating the chip formation phenomenon while performing slot milling in the aluminium nanocomposite. The effects of the selected cutting velocity

and feed on chip morphology can be visualized in 3D FE simulations. The chip morphology is mainly influenced by the shearing effect of the tool with the MMC, variety of chips with different varieties [12] are obtained for respective cutting velocity and feed combinations which can be visualised in Figure 5.

The chip flows out of the workpiece through the flute region and it breaks into small curled chips. These small curled 'C' shaped chips are observed for most of the machining parameter combinations which is due to the effect of the interaction of the plastically deformed chip with the rake surface of the end mill cutter. However, the cutting velocity and feed highly influence the chip size, shape and thickness. Moreover, nano-sized particle reinforcement enhances the yield property of the aluminium matrix [15,16] and thereby plastic deformation occurs easily resulting in the formation of 'C' and 'S' shaped curled chips which are witnessed in experimental as well as 3D FEM simulation (shown in Figures 4 b).

Chip characteristics

Chip morphology and chip formation pattern directly influence the dimensional accuracy, quality and reliability of the milling operation. Therefore, the effects of cutting velocity and feed on chip generation is to be witnessed for better understanding of chip formation and to facilitate in machining defect free components. Moreover, the tool geometry also significantly influences the chip characteristics.

Figures 5 and 6 show samples of chips collected from experimental slot milling for various machining parameter combinations. It is witnessed that chips collected are mostly 'C' shaped with a wider range of size, thickness and length which is mainly influenced by the machining parameter combination selected for slot milling. The formation of a shorter 'C' shaped chip is predominant, which is mainly due to the reinforcement of nSiCp. **The even distribution of nano SiC particles in the aluminium nanocomposite improves its ductile behaviour, which causes plastic deformation during milling followed by the generation of curved and twisted chips.** It is also observed that the chip thickness decreases while increasing the cutting velocity. However, chip thickness increases when the feed rate is increased. Chip with lamella structure is observed when $N = 250$ rpm and $f = 250$ mm/min since the thickness of the chip generated is comparatively higher. **Moreover, the stress plots of the chips show highly strained bands across the chips which mainly contributes to the formation of lamellar structure in the milled chips. The localization of very high plastic Von Mises stress bands is the major contributor to these highly strained bands which results in lamella structure formation [15].**

Figure 6 (a) shows the magnified view (5X) of the milled chip at $f = 50$ mm/min and $N = 250, 500, 1000$ rpm. The chips collected from the slot milling experiments for this particular feed rate mostly reveal very thin, curled and 'C' shaped morphology. Cracks with saw tooth were observed in

these “C” shaped chips which is because of the shearing action of the end mill cutter with the aluminium nanocomposite. Figure 6 (a) shows the magnified photographic images (5X) of the milled chip, $f = 150$ mm/min and $N = 250, 500, 1000$ rpm. In this case, the chip formation is short and thin shaped with lamella structure with cracks and saw tooth. Mostly the milled chips possess ‘C’ or ‘S’ shaped morphology, which is due to the influence of the increased feed rate when compared to the previous machining parameter conditions [12] for slot milling experimentation. Figure 6 (a) displays the magnified image (5X) of the milled chip at $f = 250$ mm/min. The milled chips show very good lamella structure at $N = 250$ rpm which is due to the effect of higher chip thickness. **At $N = 1000, 1500$ rpm the chips show twisted and rolled shaped morphologies.**

Figure 5

Figure 6

The chips collected from experimental slot milling show good similarity when correlated with the chip plots captured from 3D FE simulation results as shown in the Figure 6 b. The chip images obtained from experimental and 3D FE-based simulations show good similarity. **The displayed images reveal the presence of cracks, lamella structure and saw tooth.** This ensures that 3D FEM-based simulations well exhibit the actual slot milling process and it is also significant in investigating the complex milling operation in a cost-effective and time-consuming way instead of arduous cutting experiments [11, 48]. The chip images displayed below show the reliability and effectiveness of 3D FE simulation in predicting the chip morphology in slot milling of AA 7075 + 1.5% nSiCp nanocomposites.

The dimensions of the milled chip play a major role in enhancing the accuracy, surface finish and quality of the machined component. The length of the milled chips for most of the cutting conditions is in the 5 to 8 mm range, which is observed from both experimental and 3D FEM simulation results. The cutting depth used in the current research is 1 mm and hence the width of the chips is uniform around 1 mm for all the machining conditions. The experimentation and 3D Fem results reveal that the cutting parameters such as spindle speed and feed rate do not influence much on chip dimensions. However, the chip thickness varies with respect to cutting speed and feed rate. For higher cutting speeds the thickness of the chip reduces relatively and the chip is fragile.

Future Scope of Study

This research work encourages the researchers and industry to focus more on developing optimistic and reliable 3D FE models to perform machining simulations, which could ease the machining process and make it cost-effective and time-saving. In addition, the 3D FEMs are also

capable of estimating critical cutting force, chip characteristics and cutting stress even for worn-out tools and complex tool geometries. Hence this research work can be extended in future to investigate further with new tool geometries, MMCs and other machining operations, which could provide an insight for the industries and researchers.

CONCLUSIONS

The experimental and 3D FEM simulation studies of the slot milling operation were carried out and investigated in aluminium nanocomposite. The 3D FE simulation outcomes are compared with the experimental data for 3D FE model validation. The validated 3D FE model was utilised to perform simulation studies in slot milling of aluminium nanocomposites and it was found to be more reliable and accurate.

Experimental results show that critical cutting force (F_x and F_y) rises when the cutting velocity is reduced. However, when cutting velocity is increased the reduction of critical cutting force is observed, critical cutting force recorded is $F_y = 2080$ N for $V_c = 7.85$ m/min and $f = 250$ mm/min. The low cutting feed and higher cutting velocity are suggested to minimise the milling-induced damages. The cutting force signals predicted by the 3D FEM correlates 85 to 90 % with experimental data.

The maximum shear stress, $S_{12} = 175$ MPa and von Mises stress, $S = 459$ MPa were observed at tool - MMC interface region. The chip morphology studies disclose the mode of failure in the milled chips. The chip images captured from 3D FE simulations showed a good correlation with the milled chips. The correlation studies of experimental investigations and 3D FEM-based machining simulations prove the accuracy & reliability of the developed 3D FEM. This 3D FEM could assist researchers and industries in selecting appropriate machining parameter settings to achieve defect-free machining without any machining-induced damages. Moreover, it reduces the machining trials, time and cost.

Acknowledgements

The authors are extremely thankful to the Department of Production Engineering, Madras Institute of Technology, Chrompet for facilitating us with the required machinery and testing facility for this research work.

Nomenclature

- A - yield strength of the material, (MPa)
- B - hardening modulus, (MPa)
- n - coefficients related to strain hardening, (MPa)
- C - strain rate sensitivity coefficient
- m - temperature sensitivity coefficient
- T - temperature of the parts ($^{\circ}$ C)
- T_r - ambient temperature ($^{\circ}$ C)

T_m - melting temperature ($^{\circ}\text{C}$)
 D - material constant
 Σ - flow stress, (MPa)
 σ_1 - maximum principal stress, (MPa)
 S - maximum Von Mises stress (MPa)
 τ - shear stress, (MPa)
 μ - coefficient of friction
 τ_n - frictional stresses, (MPa)
 σ_n - normal stresses, (MPa)
 σ - Johnson-Cook flow stress, (MPa)
 ε - equivalent plastic strain
 ε_1 - equivalent plastic strain rate, (S^{-1})
 ε_0 - reference equivalent plastic strain rate, (S^{-1})
 N - spindle speed, (rpm)
 V_c - cutting velocity, (m/sec)
 f - feed rate, (mm/min)
 F_x - infeed force
 F_y - cross feed force
 F_z - thrust force

References

1. A. Macke, B.F. Schultz, P. Rohatgi, *Adv. Mater. Processes* 170(3) (2012) 19-23. <https://doi.org/10.31399/asm.amp.2012-03.p019>.
2. N. Shetty, S.M. Shahabaz, S.S. Sharma, S. Divakara, Shetty, *Compos. Struct.* 176 (2017) 790-802. <https://doi.org/10.1016/j.compstruct.2017.06.012>.
3. D. Giugliano, N.K. Cho, H. Chen, L. Gentile, *Compos. Struct.* 218 (2019) 204-216. <https://doi.org/10.1016/j.compstruct.2019.03.030>.
4. R. Bach, *Aluminium in transport* (2020)
Available from: <https://www.aluminiumleader.com/application/transport/> [accessed 16th August 2024]
5. Y. Peng, H. Zhao, J. Ye, M. Yuan, L. Tian, Z. Li, Z. Wang, J. Chen, *Compos. Struct.* 288 (2022) 115425. <https://doi.org/10.1016/j.compstruct.2022.115425>.
6. X.D. Nong, Y.L. Jiang, M. Fang, L. Yu, C.Y. Liu, *Int. J. Heat Mass Transfer* 108 (2017) 1374-1382. <https://doi.org/10.1016/j.ijheatmasstransfer.2016.11.108>.
7. K. Palanikumar, N. Muthukrishnan, K.S. Hariprasad, *Mach. Sci. Technol.* 12(4) (2008) 529-545. <https://doi:10.1080/10910340802518850>.
8. K. Giasin, A. Hodzic, V. Phadnis, S. Ayvar- Soberanis, *Int. J. Adv. Manuf. Technol.* 87(5) (2016) 2041–2061. <https://doi:10.1007/s00170-016-8563-y>.
9. M. Aamir, K. Giasin, M. Tolouei-Rad, A. Vafadar, *J. Mater. Res. Technol.* 9(6) (2020) 12484-12500. <https://doi.org/10.1016/j.jmrt.2020.09.003>.
10. M. Bhuvanesh Kumar, R. Parameshwaran, K. Deepandurai, S.M. Senthil, *Trans. Indian Inst. Met.* (2020). <https://doi.org/10.1007/s12666-020-01960-6>.
11. W. Ma, R. Wang, X. Zhou, X. Xie, *Proc. Inst. Mech. Eng., Part B* 235(1-2) (2021) 265-277. <https://doi:10.1177/0954405420932442>.
12. A. Davoudinejad, G. Tosello, P. Parenti, M. Annoni, *Micromachines* 8(6) 187 (2017). <https://doi.org/10.3390/mi8060187>.
13. P. Raghuvaran, M. Suresh, S. Aakash, M. Balaji, K. Dinesh Kumar, S. H. Prasath, *IOP Conf. Ser. Mater. Sci. Eng.* 995 (2020). <https://doi.org/10.1088/1757-899X/995/1/012040>.

14. K.H. Cui, C.Z. Ren, G. Chen, Key Eng. Mater. (589–590) (2013) 3-7. <https://www.scientific.net/KEM.589-590.3>.
15. U. Usama, A. Hisham, H.A. Mustufa, M.M. Khan, H.A. Kishawy, Adv. Mech. Eng. 13 (2021). <https://doi.org/10.1177/16878140211070446>.
16. U. Umer, M.H. Abidi, J.A. Qudeiri, H. Alkhalefah, Mater. Today: Proc. 44 (2021) 764-770. <https://doi.org/10.1016/j.matpr.2020.10.679>.
17. L. Zhou, C. Cui, P. Zhang, Int. J. Adv. Manuf. Technol. 91 (2017) 1935–1944. <https://doi.org/10.1007/s00170-016-9933-1>.
18. C. Prakash, K.S. Vijay Sekar, J. Balk. Tribol. Assoc. 23(3) (2017) 497-514.
19. C. Prakash, A. Arockia Selvakumar, J. Prakash, AIP Conf. Proc. 3216(1) (2024) 040002. <https://doi.org/10.1063/5.0226489>
20. A.F.V. Pedroso, N.P.V. Sebbe, R.D.F.S.Costa, M.L.S. Barbosa, R.C.M. Sales-Contini, F.J.G. Silva, R.D.S.G. Campilho, A.M.P. de Jesus, An Extended Review. J. Manuf. Mater. Process. 8(1) (2024) 37. <https://doi.org/10.3390/jmmp8010037>
21. S. Dodla, K.J Kirpalani Idnani, A. Katyal, Mater. Today: Proc. (2021). <https://doi.org/10.1016/j.matpr.2021.01.136>.
22. S. Deshmukh, G. Joshi, A. Ingle, D. Thakur, Mater. Today: Proc. 46 (2021) 8410-8416. <https://doi.org/10.1016/j.matpr.2021.03.450>.
23. Z. Liangchi, Wu. Zhonghuai, Wu. Chuhan, Wu. Qi, Compos. B Eng. 241, (2022) 110023, <https://doi.org/10.1016/j.compositesb.2022.110023>.
24. C. Prakash, K.S. Vijay Sekar, Adv. Sci., Eng. Med. 10(3) (2018) 308-312. <https://doi.org/10.1166/asem.2018.2125>.
25. C. Prakash, K.S. Vijay Sekar, J. Braz. Soc. Mech. Sci. Eng. 40(6) (2018) 279. <https://doi.org/10.1007/s40430-018-1195-4>.
26. C. Prakash, K.S. Vijay Sekar, IOSR J. Eng. (2018) 22-28. <https://iosrjen.org/Papers/ICPRASET%202K18/surya/Volume%201/auto/5.%2022-28.pdf>
27. C. Prakash, K.S. Vijay Sekar, Lect. Notes Mech. Eng. (2019) 81-89. https://doi.org/10.1007/978-981-13-1724-8_8.
28. C. Prakash, K.S. Vijay Sekar, IOP Conf. Ser. Mater. Sci. Eng. (2021). <https://doi.org/10.1088/1757-899X/1128/1/012050>.
29. C. Prakash, A. Arockia Selvakumar, K.S. Vijay Sekar, Mater. Today: Proc. (2023). <https://doi.org/10.1016/j.matpr.2023.08.234>.
30. C. Prakash, Int. J. Interact. Des. Manuf. (2024). <https://doi.org/10.1007/s12008-024-02089-2>
31. J. Prakash, S. Gopalakannan, Silicon 13 (2021) 409-432. <https://doi.org/10.1007/s12633-020-00434-0>.
32. J. Prakash, S. Gopalakannan, V.K. Chakravarthy, Silicon 14(4) (2022) 1683-1694. <https://doi.org/10.1007/s12633-021-00979-8>.
33. H. Liu, W. Zhu, H. Dong, Ke. Yinglin, Mechatronics 46 (2017) 101–114. <https://doi.org/10.1016/j.mechatronics.2017.07.004>.
34. R.K. Bhushan, Adv. Compos. Hybrid Mater. 4(1) (2021) 74-85. <https://doi.org/10.1007/s42114-020-00175-z>.
35. I. Boughdiri, T. Mabrouki, R. Zitoune, K. Giasin, M.F. Ameer, Compos. Struct. 304 (2023) 116458. <https://doi.org/10.1016/j.compstruct.2022.116458>.
36. T.Ozben, E. Kilickap, O.Çakır, J. Mater. Process. Technol. 198(1–3) (2008) 220-225. <https://doi.org/10.1016/j.jmatprotec.2007.06.082>.

37. S.Deshmukh, G. Joshi, A. Ingle, D.S. Thakur, Mater. Today: Proc. 46(17) (2021) 8410-8416. <https://doi.org/10.1016/j.matpr.2021.03.450>.
38. S.S. Babu, C. Dhanasekaran, G. Anbuezhayan, K. Palani, Eng. Res. Express. 4 (2022) 025036. <https://doi.org/10.1088/2631-8695/ac7038>.
39. D. Simulia, Abaqus 6.14 User's manual (2014) Dassault systems. <http://50.16.225.63/v6.14/>
40. CATIA V5R14, User Manual (2014) Dassault systems. https://www.maruf.ca/files/catiahelp/CATIA_P3_default.htm
41. T. Mabrouki, F. Girardin, M. Asad, J.F. Rigal, Int. J. Mach. Tools Manuf. 48 (2008) 1187–97. <https://doi.org/10.1016/j.ijmachtools.2008.03.013>.
42. C. Prakash, J. Prakash, Proc. Inst. Mech. Eng., Part D (2024). <https://doi.org/10.1177/09544070241254148>.
43. G. Johnson, W. Cook, Eng. Fract. Mech. 21(1) (1985) 31–48. [https://doi.org/10.1016/00137944\(85\)90052-9](https://doi.org/10.1016/00137944(85)90052-9).
44. S. Rasaei, A.H. Mirzaei, D. Almasi, Bull. Mater. Sci. 43(1) (2020) 1-8. <https://doi.org/10.1007/s12034-019-1987-x>.
45. J.Y. Sheikh-Ahmad, Textbook of Machining of Polymer Composites, Springer New York, NY (2009). <https://doi.org/10.1007/978-0-387-68619-6>.
46. H. Yu, Z. He, J. Li, Int. J. Adv. Manuf. Technol. 124 (2023) 97–110. <https://doi.org/10.1007/s00170-022-10476-w>.
47. G. Li, M. Liu, S. Zhao, Mach. Sci. Technol. 25(4) (2021) 558–584 <https://doi.org/10.1080/10910344.2020.1855651>.
48. C. Prakash, J. Prakash, Arch. Metall. Mater. 70(2) (2025) [Accepted article].

Table captions

Table 1. Machining parameters settings for experimental slot milling of Aluminium Nano composite

Table 2. 3D FEM - Input data

Table 3. Chemical composition, Mechanical properties, J-C parameters and Damage criteria of aluminium nano composite [17, 25].

Table 4. Critical Cutting Force data recorded for various cutting velocities and cutting feed combinations.

Table 1.

Machining parameters	Values
Spindle speeds, N (rpm)	250, 500, 1000, 1500
Cutting Velocity, V_c (m/min)	7.85, 15.7, 31.4, 47.1
In feed rate, f (mm/min)	50, 150, 250
Slot depth (mm)	1

Table 2.

Work Piece	Aluminium nanocomposite
Tool	End Mill cutter – 10 mm Diameter
Dimensions of Workpiece (MMC)	25 X 25 X10 mm
Element type for MMC	C3D8R
Number of elements in MMC	50,000
Number of nodes in MMC	54,621
Element Size in MMC	0.25 mm
Type of Element in End mill	C3D10M
Number of elements in End mill	32,895
Number of nodes in End mill	49,665
Element Size in End mill	1 mm
Total Elements & Nodes in 3D FEM	82,895 & 1,04,286
Friction Factor	0.6 & Coulomb Friction [35]
Damage initiation	1E-4
Failure Criteria	Johnson - Cook Model

Table 3.

Composition of aluminium nanocomposite – AA7075 + 1.5% nSiCp (percentage by weight) [27, 28]										
Cr	Mg	Zn	Cu	Si	Mn	Ti	Fe	SiC	Al	
0.2	2.4	5.7	2.0	0.3	0.1	0.1	0.22	1.5	Bal	
Mechanical Properties of the composite [25]										
Specifications			Value(s)	Specifications			Value(s)			
Modulus of Elasticity, E (GPa)			71	Tensile Strength (MPa)			285.64			
Poisson's ratio			0.27	Yield Strength (MPa)			245.12			
Thermal Expansion Coefficient, (1/K)			23.6 E-6	Ultimate Strength (MPa)			260.56			
Thermal Conductivity, k (W/mK)			180	Shear Strength (MPa)			150.53			
Specific heat (J/kg K)			880	Density of the composite (kg/m3)			2790			
Johnson – Cook parameters [35]										
A (MPa)	B (MPa)	n	m	C	Temperature, T (K)	Damage Initiation				
251	1443	0.749	1.571	0.0166	305	0.001				
Damage Parameters										
d ₁		d ₂		d ₃		d ₄		d ₅		
-0.77		1.45		-0.47		0		1.60		

Table 4.

Feed, f (mm/min)	Cutting Velocity, V_c (m/min)	Critical cutting force (N)					
		In Feed (F_x)		Cross Feed (F_y)		Thrust force (F_z)	
		Expt.	FEA	Expt.	FEA	Expt.	FEA
50	7.85	638	647	785	792	118	122
	15.7	353	361	451	462	69	73
	31.4	235	246	275	286	49	46
	47.1	157	162	196	206	39	34
150	7.85	716	719	746	759	167	156
	15.7	765	754	608	619	118	111
	31.4	579	586	481	493	59	57
	47.1	530	524	451	464	49	48
250	7.85	1511	1526	2080	2099	88	86
	15.7	1373	1392	1668	1679	59	55
	31.4	1305	1328	1305	1321	39	34
	47.1	1099	1086	1040	1062	29	27

Figure captions:

Figure 1: a) Stir-casting with ultrasonic cavitation setup [25]; b) FESEM micrograph of the composite [25]; c) Milling experiment set up with Data - acquisition system

Figure 2: a) Three dimensional model of the solid carbide end mill cutter; b) Three dimensional Finite Element Model of end milling aluminium nanocomposite

Figure 3: a) Comparison of experimental and 3D FEM cutting force (F_x) during slot milling of aluminium nanocomposite when $V_c = 47.1$ m/min and $f = 150$ mm/min; b) Comparison of experimental and 3D FEM cutting force (F_y) during slot milling of aluminium nanocomposite when $V_c = 47.1$ m/min and $f = 150$ mm/min; c) Cutting velocity and Feed rate Vs. Critical cutting force (F_x); d) Cutting velocity and Feed rate Vs. Critical cutting force (F_y)

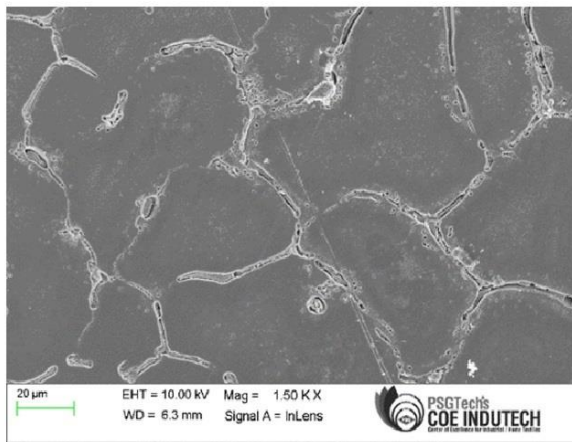
Figure 4: a) Stress Plots from 3D FEA simulation when $V_c = 15.7$ m/min and Feed rate = 50 mm/min; b) 3D FEA Slot Milling Simulation of chip formation at $V_c = 15.7$ m/min, Feed rate = 50 mm/min

Figure 5: Chip Morphology of aluminium nanocomposite while slot milling with different cutting parameter combinations

Figure 6: a) Experimental chip characteristics at different spindle speed and feed; b) Comparison of Chips morphology - Experimental results Vs. 3D FE simulation results



(a)

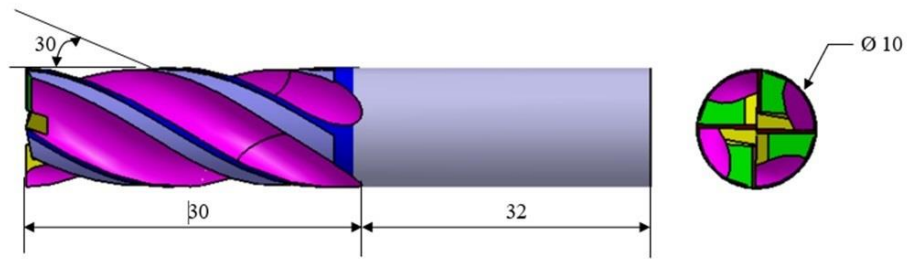


(b)

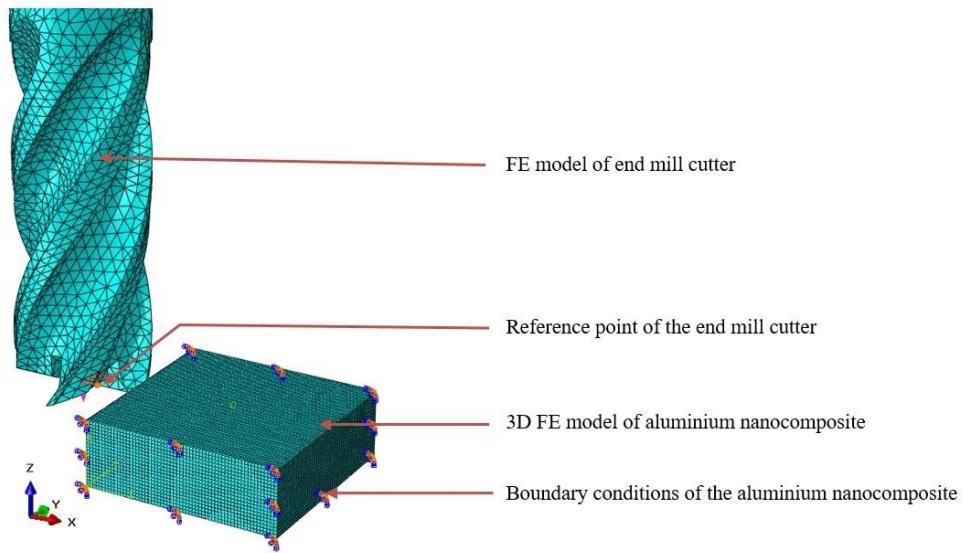


(c)

Figure 1

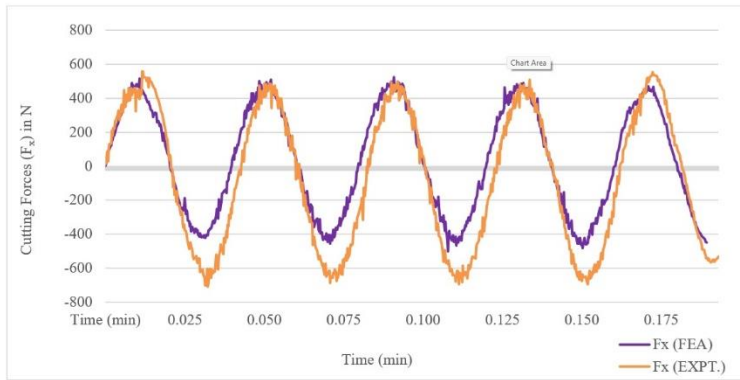


(a)

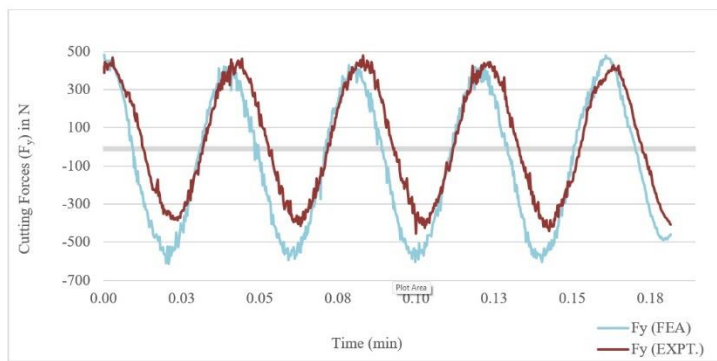


(b)

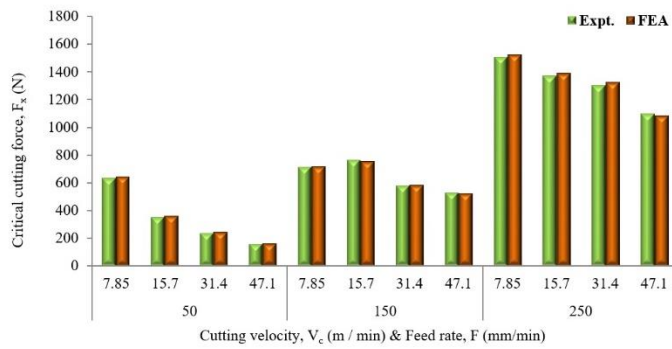
Figure 2



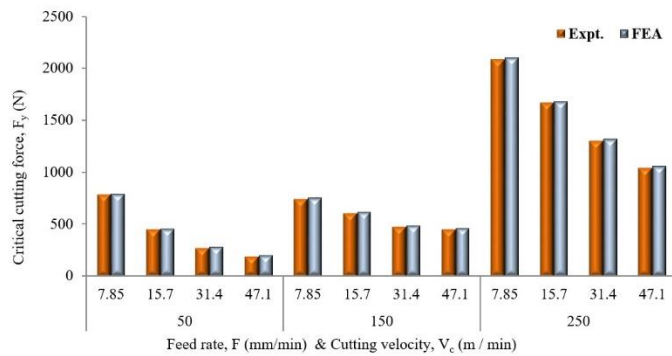
(a)



(b)

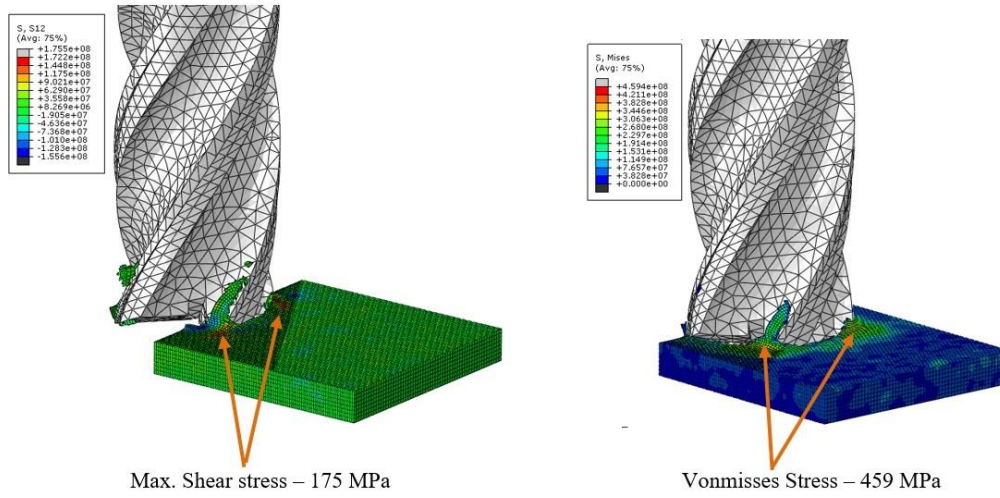


(c)

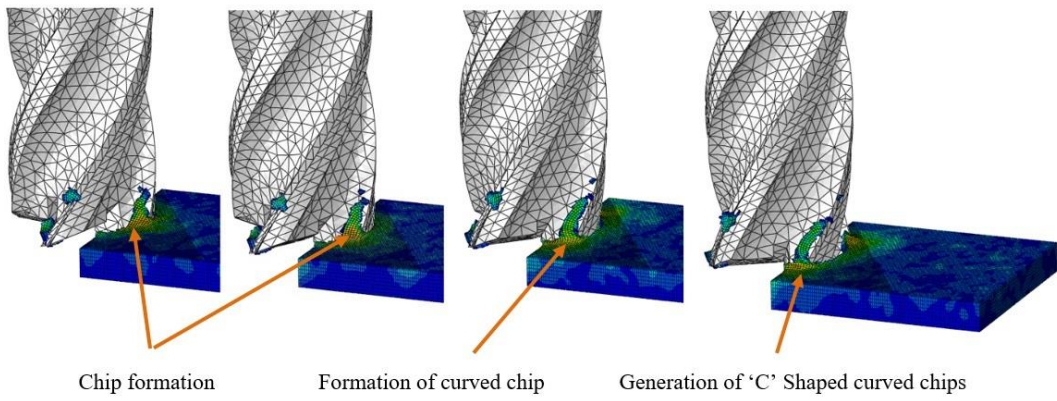


(d)

Figure 3



(a)



(b)

Figure 4











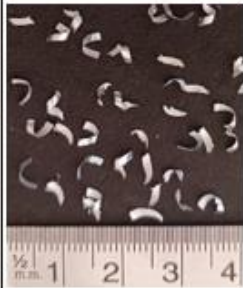

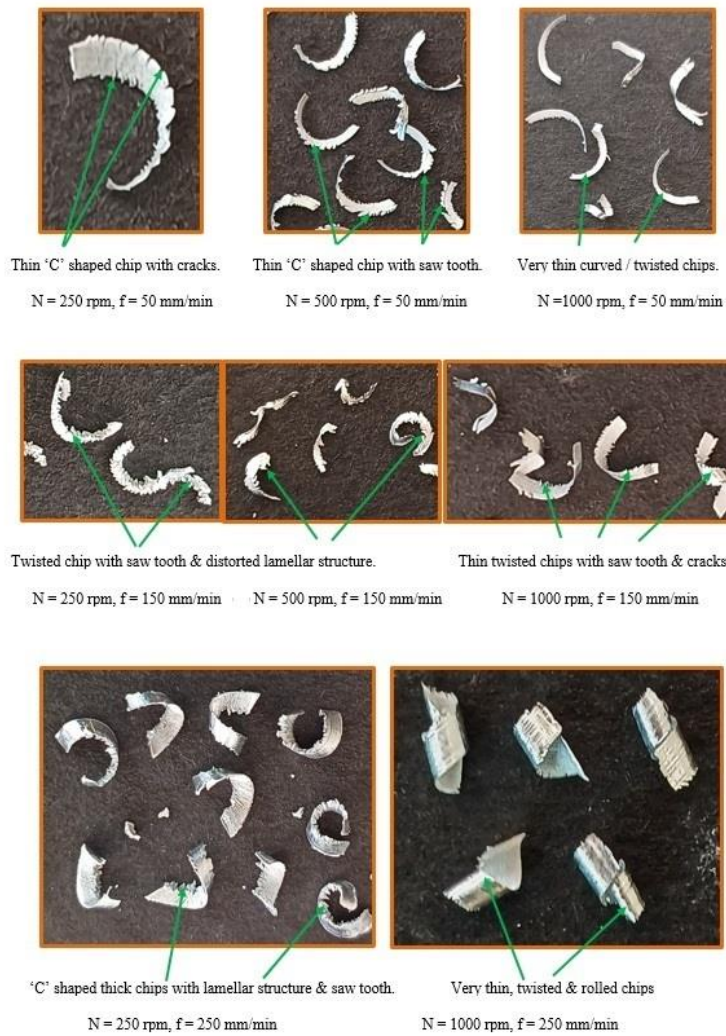
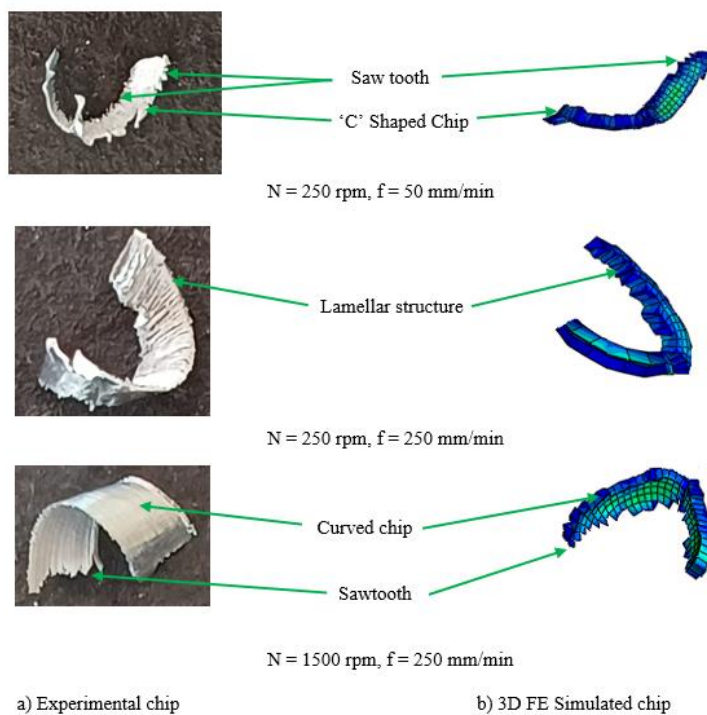
Spindle Speed (rpm)	Feed rate (mm/min)		
	50	150	250
250			
500			
1000			
1500			

Figure 5.



(a)



(b)

Figure 6